J Bioenerg Biomembr (2006) 38:1–10
DOI 10.1007/s10863-006-9000-y

ORIGINAL PAPER

Role of mitochondria in the immune response to cancer: a central role for Ca^{2+}

Giovanna R. Degasperi · Jesus A. Velho · Karina G. Zecchin · Cláudio T. Souza · Lício A. Velloso · Jiri Borecký · Roger F. Castilho · Anibal E. Vercesi

Received: 28 December 2005 / Accepted: 8 January 2006 / Published online: 16 June 2006

Abstract This study demonstrates that Ca^{2+} stimulates mitochondrial energy metabolism during spleen lymphocyte activation in response to the ascitic Walker 256 tumor in rats. Intracellular Ca^{2+} concentrations, phosphorylated protein kinase C (pPKC) levels, Bcl-2 protein contents, interleukin-2 (IL-2) levels, mitochondrial uncoupling protein-2 (UCP-2) contents and reactive oxygen species (ROS) were significantly elevated in these activated lymphocytes. Mitochondria of activated lymphocytes exhibited high free Ca^{2+} concentrations in the matrix and enhanced oligomycin-sensitive oxygen consumption, indicating an increased rate of oxidative phosphorylation. The production of ROS was largely decreased by diphenylene iodinium in the activated lymphocytes, suggesting that NADPH oxidase is the prevalent source of these species. Accumulation of UCP-2 and the anti-apoptotic protein Bcl-2 is probably important to prevent mitochondrial dysfunction and cell death elicited by the sustained high levels of intracellular Ca^{2+} and ROS and may explain the observed higher resistance from activated lymphocytes against the opening of the mitochondrial membrane permeability pore (MPT). All these changes were blocked by pretreatment of the rats with verapamil, an L-type Ca^{2+} channel antagonist. These data demonstrate a central role of Ca^{2+} in the control of mitochondrial bioenergetics in spleen lymphocytes during the immune response to cancer.

Keywords Calcium homeostasis · Cancer · Lymphocyte activation · Mitochondria · Oxidative stress · Verapamil

G. R. Degasperi · J. A. Velho · K. G. Zecchin · J. Borecký · R. F. Castilho · A. E. Vercesi (✉)
Departamento de Patologia Clínica, Faculdade de Ciências Médicas, Universidade Estadual de Campinas (UNICAMP), Campinas, SP 13083-970, Brazil
e-mail: anibal@unicamp.br

C. T. Souza · L. A. Velloso
Departamento de Clínica Médica, Faculdade de Ciências Médicas, Universidade Estadual de Campinas (UNICAMP), Campinas, SP 13083-970, Brazil

Introduction

Immune system responses to cancer include lymphocyte activation (Michalek et al., 2004). The engagement of an antigen with the lymphocyte receptor induces a biphasic intracellular Ca^{2+} response. In the initial phase, a large elevation of the intracellular Ca^{2+} levels at the expense of intracellular stores occurs. Subsequently, a lower but prolonged elevation of Ca^{2+} levels is observed, in a manner dependent on the influx of extracellular Ca^{2+} through L-type Ca^{2+} channels sensitive to dihydropyridine antagonists such as verapamil (Birx et al., 1984; Lewis, 2001). This activates Ca^{2+}-dependent signal-transduction pathways leading to the formation of several products including nuclear factors NF-AT, AP-1, Oct-1, NF-κB and ROS (Ma et al., 2002). These nuclear factors regulate the expression of various genes encoding cytokines, mainly IL-2 (Allen and Tresini, 2000; Barja, 2002; Dröge, 2002; Finkel and Holbrook, 2000) that promotes cell cycle progression (Ma et al., 2002). ROS, mainly H_2O_2, stimulate the immunological cascade of lymphocyte activation by inhibiting protein tyrosine phosphatases via oxidation of their cysteine residues located at the catalytic site (Reth, 2002).

NADPH oxidase and mitochondria are the main cellular sources of ROS generation (Halliwell and Gutteridge, 1999). Therefore, both systems could contribute to ROS production

during lymphocyte activation. NADPH oxidase is dormant in resting cells but is functional in activated lymphocytes and phagocytes. PKC promotes NADPH oxidase activation through phosphorylation of $p47^{PHOX}$, a subunit of NADPH oxidase located in the cytosol of resting cells (Fontayne et al., 2002). Phosphorylated $p47^{PHOX}$ then migrates to the plasma membrane, where it combines with another subunit of NADPH oxidase, cytochrome b_{558}, and leads to lymphocyte activation (Park et al., 1997).

Mitochondrial ROS generation is stimulated under conditions of low energy demand in which low oxygen consumption rates render a more reduced state of respiratory chain components, favoring electron transfer to $\mathbf{O_2}$ by complexes I and III, which generates $O_2^{\cdot -}$ (Boveris and Fraga, 2004). ROS release is prevented by high respiratory rates during oxidative phosphorylation or increased expression and activity of mitochondrial UCPs and ATP-sensitive K^+ channels, which enhance respiration in the absence of oxidative phosphorylation (Ferranti et al., 2003; Kowaltowski et al., 1998; Mattiasson et al., 2003; Negre-Salvayre et al., 1997). Indeed, $O_2^{\cdot -}$ and H_2O_2 activate UCPs perhaps as a negative feedback system to control mitochondrial ROS release (Echtay et al., 2002). In this respect, it has been suggested that UCP-2 is involved in immunity and inflammatory response (Arsenijevic et al., 2000; Horvath et al., 2003). However, its role in the pathophysiology of various diseases, including cancer, remains unclear.

Considering the high metabolic energy required for lymphocyte activation and the association of this process with oxidative stress, we analyzed changes in spleen lymphocyte mitochondrial bioenergetics in Walker 256 tumor-bearing rats. We found that Ca^{2+} mediates a mitochondrial response that allows the organelle to cope with a high energy demand and oxidative stress.

Materials and methods

Antimycin A, carbonyl cyanide m-chloro phenylhydrazone (CCCP), Cyclosporin-A, diphenylene iodinium (DPI), and oligomycin were obtained from Sigma (St. Louis, MO, USA). 3,3′-dihexyloxarbocyanine ($DioC_6(3)$), Fluo-3AM, Fura-2AM, Rhod-2AM, Pluronic acid F-127, dichlorodihydrofluorescein diacetate (H_2-DCFDA), and dihydroethidium (DHE) were purchased from Molecular Probes Inc. (Eugene, OR, USA). Ficoll-Paque™ PLUS was from Becton Dickinson Biosciences (San Jose, CA, USA), RPMI 1640 and bovine fetal serum (FBS) was from Cutilab (Campinas, Brazil), and Endogen Rat Interleukin-2 (IL-2) ELISA Kit was from Pierce Biotechnology (Rockford, IL, USA). Anti-UCP-2, and anti-Bcl-2 were obtained from Santa Cruz Biotechnology (Santa Cruz, CA, USA) and anti-phosphorylated PKC (anti-pPKC) was from Cell Signaling (Beverly, MA, USA). All other chemicals were standard commercial products of reagent-grade quality.

Animal treatment

Nine-week-old male Wistar rats (*Rattus norvegicus albinos*) were obtained from the State University of Campinas Central Animal Breeding Center. Rats were kept under standard laboratory conditions (20–22°C and 12 h/12 h day/night cycle) with free access to a standard diet and water. The investigation followed the University guidelines for the use of animals in experimental studies (protocol no. 487–1, approved by the local Ethical Committee in 2002) and was conformed to the Guide for the Care and Use of Laboratory Animals published by the US National Institutes of Health (NIH publication no. 85–23, revised in 1996).

The Walker 256 tumor cell line (originally obtained from the Christ Hospital Line, National Cancer Institute Bank, Cambridge, MA) was kept frozen in liquid nitrogen (40×10^6 cells/mL in PBS, 1% FBS, and 10% DMSO). Walker 256 cells were maintained through consecutive intraperitoneal inoculums, each containing 20×10^6 tumor cells in PBS. Walker 256 tumor cells were isolated from the ascitic fluid (see later) 4–5 days after inoculation. Verapamil (8.13 mg/kg) was administrated daily through gavage for 8–9 days, starting 4 days before the Walker 256 cell inoculation.

Isolation of Walker 256 tumor cells and spleen lymphocytes

Ascitic fluid containing tumor cells (2 mL per animal) was collected through intraperitoneal punctures. Spleens were gently homogenized in a manual Douncer homogenizer. Ascitic fluid or spleen homogenates were overlaid onto a Ficoll-Paque™ PLUS layer with density adjusted to 1.076 g/mL and centrifuged at $1000 \times g$ at room temperature for 25 min. The interface cell layer was recovered with a Pasteur pipette, washed twice in PBS and centrifuged at $500 \times g$ for 10 min (Böyum, 1968). Cells were counted using a Neubauer chamber, using trypan blue to mark dead cells. Cells were used when the viability was >98%.

Flow cytometry analysis

The samples were analyzed in a FACSCalibur flow cytometer equipped with an argon laser and CellQuest software. Ten thousand events were collected for each sample. The lymphocyte populations were identified by their light-scattering characteristics, enclosed in electronic gates, and analyzed for the intensity of the fluorescent probe signal.

Concentration of IL-2

The concentration of endogenous IL-2 in spleen lymphocytes was measured with the Endogen Rat Interleukin-2 ELISA Kit according to the manufacturer's recommended procedure. Absorbance at 370 nm was determined with a microplate reader (Labsystems Multiskan MS type 352, Helsinki, Finland).

Determination of the mitochondrial electrical transmembrane potential ($\Delta\Psi_m$) in intact lymphocytes

Lymphocytes (10^6 cells/mL) were incubated with 0.2 nM iodide $DioC_6(3)$, with or without 1 μg/mL oligomycin, in 400 μL of RPMI 1640 medium supplemented with 1% FBS at 37°C in a humidified CO_2 incubator (5% CO_2) for 30 min. One half of each cell sample (200 μL) was separated into a new tube, where 50 μM CCCP was added. Both halves of samples were incubated for further 30 min prior to analysis by flow cytometry. $DioC_6(3)$, at nonsaturating concentration, binds preferentially to mitochondria, since the magnitude of mitochondrial electrical membrane potential is much higher (−180 mV) than plasma membrane potential (−60 mV). Results from experiments in triplicate were normalized using F/F_{CCCP} ratio where F is the mean fluorescence intensity of $DioC_6(3)$ (maximum fluorescence) and F_{CCCP} is the mean fluorescence intensity in the presence of CCCP (minimum fluorescence). CCCP, a protonophore, dissipates the mitochondrial electrical membrane potential (Rottenberg and Wu, 1998).

Determination of $\Delta\Psi_m$ in digitonin-permeabilized lymphocytes

$\Delta\Psi_m$ in digitonin-permeabilized spleen lymphocytes was estimated as fluorescence changes of safranin O (Akerman and Wikstron, 1976) recorded using a spectrofluorometer (Hitachi, model F–4500) operating at excitation and emission wavelengths of 495 and 586 nm, respectively, with slit widths of 2.5 nm. Spleen lymphocytes (10^7 cells/mL) were permeabilized with 0.001% digitonin (Fiskum et al., 1980) in 2.0 mL of standard reaction medium (125 mM sucrose, 65 mM KCl, 10 mM HEPES-Na buffer, pH 7.2, 1 mM $MgCl_2$, 2 mM potassium phosphate, 5 mM succinate, 20 μM EGTA and 10 μM safranin O) under constant stirring at 37°C. The results are representative of at least three independent experiments.

Determination of oxygen consumption

Oxygen consumption was measured using a Clark-type electrode (Hansatech Instruments Limited, Norfolk, UK) in RPMI 1640 (37°C) containing 200 μM EGTA plus 1% FBS, in a 0.5 mL (15×10^6 cells/mL) thermostated sealed glass cuvette equipped with a magnetic stirrer. Other additions are indicated in the figure legends.

Quantification of adenine nucleotides

Adenine nucleotides were quantified by anion-pair-reversed-phase chromatography method (Manfredi et al., 2002) using a solution of 100 mM KH_2PO_4, 5 mM tetrabutylammonium bromide, and 2% CH_3CN, adjusted to pH 3.3 with H_3PO_4, as a mobile phase. Samples of spleen lymphocytes (15×10^6 cells/mL) were derivatized with chloroacetaldehyde and fluorescence of adenine nucleotides were detected by liquid chromatography system LC-10A*vp* operated by CLASS-VP Data System software (Shimadzu). A run time of 40 min was used for each sample. Flow rates were maintained at 1.0 mL/min and chromatograms were recorded at the excitation/emission wavelength pair of 270/410 nm.

Measurement of intracellular ROS levels

Intracellular ROS generation was assessed using 1 μM H_2DCFDA. Lymphocyte samples (15×10^6 cells/mL) were incubated in standard reaction medium (50 mM sucrose, 65 mM KCl, 10 mM HEPES-Na buffer, pH 7.2, 2 mM $MgCl_2$, 2 mM sodium phosphate, and 5 mM succinate) under constant stirring at 37°C. The fluorescence signal was recorded at the excitation/emission wavelength pair of 488/525 nm using a fluorimeter (Hitachi, model F4500). Calibration was performed with known concentrations of (dichlorofluorescein) DCF, the product of H_2-DCF oxidation (Maciel et al., 2001). Alternatively, ROS production was measured by flow cytometry using the probe DHE. Lymphocytes (10^6 cells/mL) were preincubated in RPMI 1640 medium containing 3 μM DHE at 37°C in a humidified CO_2 incubator (5% CO_2) for 40 min.

UCP-2, Bcl-2 and pPKC detection

Spleen lymphocytes were lysed in a buffer containing 100 mM Tris–HCl (pH 7.5), 10 mM EDTA, 10% SDS, 100 mM NaF, 10 mM sodium pyrophosphate, 10 mM sodium orthovanadate, 2 mM PMSF, 0.1 mg/mL aprotinin, 1 μM pepstatin and 10% Triton X-100. Hundred micrograms of protein was separated by SDS-PAGE and transferred electrophoretically to a nitrocellulose membrane. After blocking with 5% non-fat dry milk in Tris–HCl pH 7.5 containing 150 mM NaCl and 0.1% Tween-20 (TBST) for 4 h, the membranes were probed at room temperature for 2 h with the following polyclonal antibodies: anti-UCP-2 (1:700), anti-Bcl-2 (1:500) and anti-pPKC (pan) (1:500). After the addition of respective HRP-conjugated secondary

antibodies, the reactions were developed with an enhanced chemiluminescent detection system (ECL Detection Kit, Amersham Biosciences, USA). The membranes were exposed to X-Omat AR Films (Eastman Kodak Co., Rochester, NY), and the results were quantified by densitometric analysis using NIH Imaging Software (Scion Image Beta 4.02, Scion Corporation, Frederick, MD) (De Souza et al., 2003).

Measurement of cytosolic free Ca^{2+} concentrations

Spleen lymphocytes (15×10^6 cells/mL) were loaded with 5 μM Fura-2 AM, a dual-wavelength radiometric indicator, in incubation medium containing 20 mM HEPES-Na buffer, pH 7.4, 120 mM NaCl, 3 mM KCl, 0.5 mM KH_2PO_4, 5 mM $NaHCO_3$, 1.2 mM Na_2SO_4, 10 mM glucose, 1.2 mM $MgCl_2$, 1.3 mM $CaCl_2$ and 30 μg/mL BSA for 40 min. Cytosolic free Ca^{2+} concentration in Fura-2-loaded lymphocytes was determined at the excitation wavelengths of 340 and 380 nm and emission wavelength of 510 nm using a fluorimeter (Hitachi, model F4500). Alternatively, changes in cytosolic Ca^{2+} concentrations ($[Ca^{2+}]_{cyt}$) were monitored with the green fluorescent probe Fluo-3AM (5 μM), a single wavelength indicator, by flow cytometry. Spleen lymphocytes (10^6 cells/mL) in RPMI 1640 medium were loaded with 5 μM Fluo-3AM containing 1 μM pluronic acid F-127 (for proper dispersal) and 30 μg/mL BSA in a humified CO_2 incubator (5% CO_2) at 37°C for 40 min. Nonhydrolyzed Fluo-3 AM was removed by washing the cells with medium just before fluorescence acquisition. Calibration was performed at the end of each experiment. $[Ca^{2+}]_{cyt}$ was calculated considering K_d of the Ca^{2+}-Fluo-3 complex and Ca^{2+}-Fura-2 390 and 225 nM, respectively (Tsien, 1998; Mather and Rottenberg, 2002).

Intramitochondrial Ca^{2+} measurements

For measurement of intramitochondrial free Ca^{2+} concentrations ($[Ca^{2+}]_{mit}$), spleen lymphocytes (10^6 cells/mL) were loaded with 5 μM Rhod-2AM in the presence of 1 μM pluronic acid F-127 and 30 μg/mL BSA in incubation medium RPMI 1640 at 4°C for 1 h. Samples were centrifuged at $2000 \times g$ for 2 min, resuspended in RPMI 1640 medium and incubated at 25°C for 30 min to allow hydrolysis of Rhod-2AM trapped in mitochondria. Rhod-2 fluorescence was determined by flow cytometry. Calibration was performed at the end of each experiment. $[Ca^{2+}]_{mit}$ was calculated considering the $K_d = 0.57$ μM (Metha and Shaha, 2004).

Statistical analysis

The results from at least five independent experiments performed in triplicate are displayed as means ± SEM. Comparisons between groups were done by ANOVA followed by post hoc analysis using Bonferroni corrected *t* test. The level of significance was set at $p < 0.05$. All data were analyzed using SYSTAT software (SYSTAT Software Inc., Richmond, CA).

Results

Intraperitoneal development of Walker 256 tumor restrains spleen lymphocytes from cell death and promotes their activation

Lymphocyte activation was assessed as a function of increasing levels of IL-2 and PKC phosphorylation, which also reflects activation of NADPH oxidase (Fontayne et al., 2002). Figure 1A shows that IL-2 levels were 2.2-fold higher in spleen lymphocytes from tumor bearing rats (TBR) than in those from control rats (CTR), suggesting that TBR lymphocytes were activated. This activation was confirmed by western blot analyses of PKC phosphorylation (Fig. 1B) that was fivefold higher in lymphocytes from TBR. Verapamil treatment of TBR almost completely eliminated the increase of both IL-2 production and PKC phosphorylation, demonstrating their tight dependence on Ca^{2+} influx through specific plasma membrane Ca^{2+} channels (Fig. 1A and B). In contrast, the treatment of control rats with verapamil did not alter the lymphocyte IL-2 production or phosphorylated PKC levels. Figure 1C shows that Bcl-2 levels were about threefold higher in spleen lymphocytes from TBR when compared to those from CTR, suggesting that the accumulation of Bcl-2 restrained lymphocytes cell death.

$[Ca^{2+}]_{cyt}$ and $[Ca^{2+}]_{mit}$ are elevated in TBR lymphocytes

The results obtained in the presence of verapamil (Fig. 1) suggest that the ascitic inoculation of Walker tumor cells promoted an increase in intracellular Ca^{2+} concentrations in spleen lymphocytes. Indeed, Fig. 2 shows that lymphocytes obtained from inoculated rats presented a two-fold increase in cytosolic free Ca^{2+} concentrations when compared to controls. This was observed in lymphocytes loaded with the fluorescent probe Fura-2 (white bars) as well as with Fluo-3 (gray bars). Moreover, free mitochondrial Ca^{2+} concentrations were threefold higher in TBR lymphocytes than in control lymphocytes (Fig. 3).

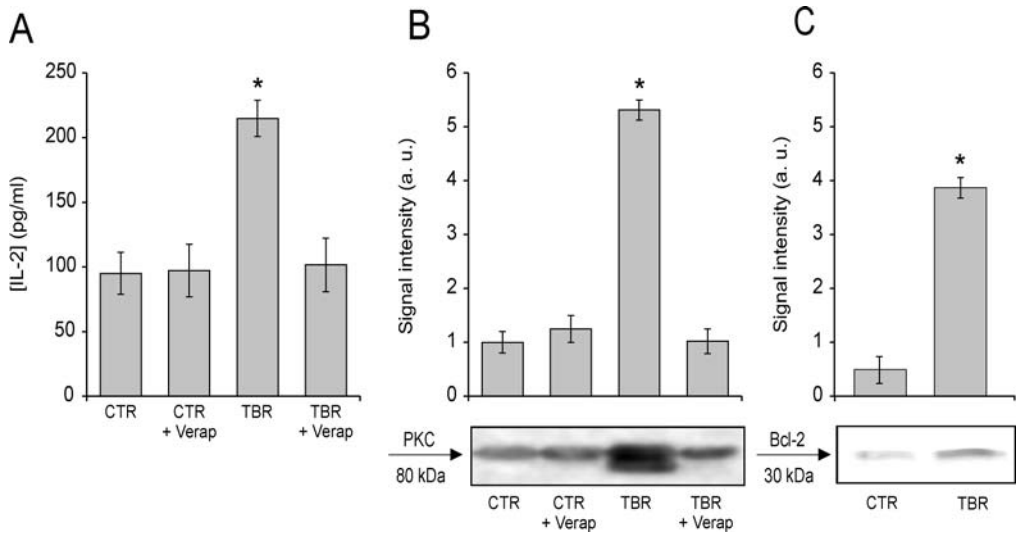

Fig. 1 Levels of IL-2, phosphorylated PKC (pPKC) and Bcl-2 proteins in spleen lymphocytes. IL-2 (A) in spleen lymphocytes (10^8 cells) was determined by ELISA. pPKC and Bcl-2 protein levels (B and C) were determined by Western blot analyses using anti-pPKC and anti-Bcl-2 antibodies performed with 100 μg of total protein extracts from lymphocytes. Data are expressed as integrated optical density (a.u.: arbitrary units) of pPKC and Bcl-2 bands (B and C, *lower panels*). Bars represent means ± SEM of five independent experiments. $^{*}p < 0.0001$ versus CTR, CTR treated with verapamil (CTR + Verap), or TBR treated with verapamil (TBR + Verap)

Addition of CCCP or oligomycin plus antimycin A, which collapses $\Delta\Psi_m$, to Rhod-2-loaded TBR lymphocytes decreased matrix Ca^{2+} concentration to levels lower than those present in CTR lymphocyte mitochondria (Fig. 3). These results indicate that mitochondria presented enhanced Ca^{2+} uptake in response to high free cytosolic Ca^{2+} concentrations. Treatment of TBR lymphocytes with verapamil abolished the increase in both free cytosolic and mitochondrial Ca^{2+} concentrations (Figs. 2 and 3).

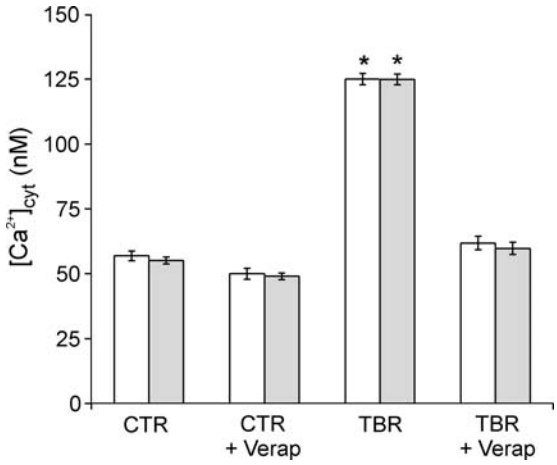

Fig. 2 Cytosolic free Ca^{2+} concentrations ($[Ca^{2+}]_{cyt}$) in spleen lymphocytes. $[Ca^{2+}]_{cyt}$ in spleen lymphocytes was measured fluometrically using Fura-2 (15×10^6 cells/mL; *white bars*) and by flow cytometry with Fluo-3 (10^6 cells/mL; *gray bars*). Bars represent means ± SEM of five independent experiments. $^{*}p < 0.001$ versus all other experimental groups

TBR lymphocytes are resistant to Ca^{2+}-induced mitochondrial permeability transition

Figure 4 shows that mitochondria within digitonin-permeabilized CTR (trace *e*) and TBR (trace *f*) lymphocytes generate and sustain a stable $\Delta\Psi_m$. Accordingly, the

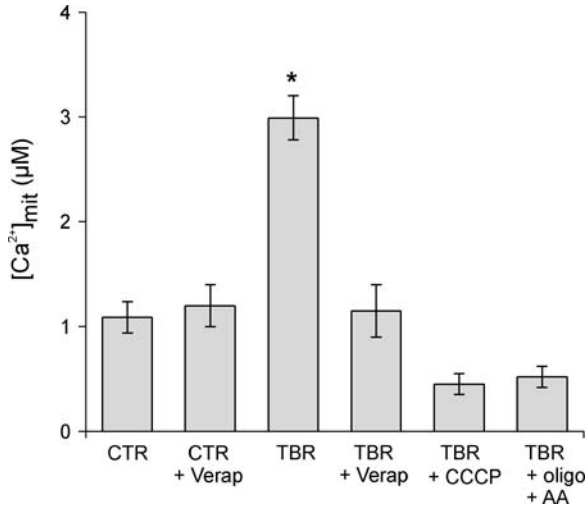

Fig. 3 Free mitochondrial Ca^{2+} concentrations ($[Ca^{2+}]_{mit}$) in spleen lymphocytes. $[Ca^{2+}]_{mit}$ in spleen lymphocytes (10^6 cells/mL) was determined with Rhod-2. Spleen lymphocytes loaded with Rhod-2 were preincubated in RPMI 1640 medium in a humidified CO_2 incubator (5% CO_2) at 37°C for 30 min before fluorescence acquisition in a flow cytometer. CCCP (2 μM) or 1 μM oligomycin plus 1 μM antimycin A (oligo + AA) were present during the preincubation period, as indicated. Bars represent means ± SEM of 5 independent experiments. $^{*}p < 0.001$ versus all other experimental groups

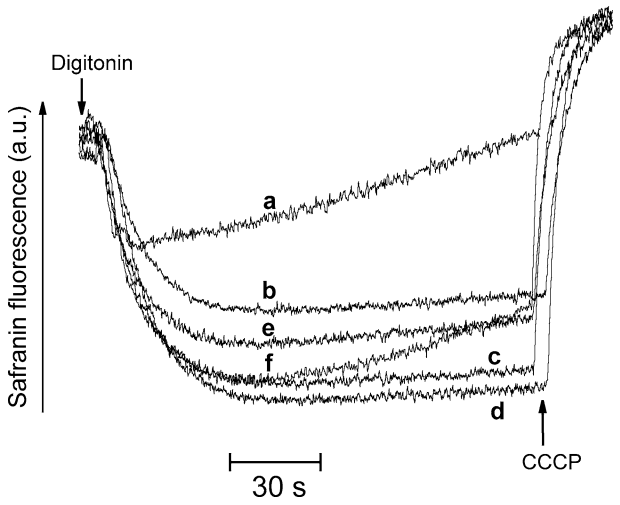

Fig. 4 TBR lymphocytes are more resistant to Ca^{2+}-induced MPT. Lymphocytes (10^7 cells/mL) were incubated under constant stirring at 37°C in 2.0 mL of medium containing 125 mM sucrose, 65 mM KCl, 10 mM HEPES buffer pH 7.2, 1 mM $MgCl_2$, 2 mM potassium phosphate, 5 mM succinate, 20 μM EGTA, and 10 μM safranin O. Experiments were conducted in the presence of 75 μM Ca^{2+} (*traces a* and *b*, CTR and TBR lymphocytes, respectively), 75 μM Ca^{2+} plus 1 μM CsA (*traces c* and *d*, CTR and TBR lymphocytes, respectively) or no other additions (*traces e* and *f*, CTR and TBR lymphocytes, respectively). Digitonin (0.001%) and 2 μM CCCP were added where indicated by the *arrows*. Traces are the representative of three independent experiments

addition of the protonophore CCCP promoted its collapse. However, when the experiments were done in the presence of Ca^{2+}, TBR mitochondria (trace *b*) generated a sustained $\Delta\Psi_m$ much larger than CTR mitochondria (trace *a*). Cyclosporin A, an inhibitor of the MPT (Crompton et al., 1988) (traces *c* and *d*) prevented $\Delta\Psi_m$ loss promoted by Ca^{2+}, indicating this loss was due to mitochondrial permeability transition.

TBR lymphocytes exhibit low ATP/ADP ratios and high rates of oxidative phosphorylation

TBR lymphocytes presented higher ADP levels and lower ATP contents than controls, resulting in decreased ATP/ADP ratios (Fig. 5). These changes in high-energy phosphate contents may be related to the high energy demand of lymphocyte activation processes. As expected, changes in ATP/ADP ratios were associated with a lower $\Delta\Psi_m$ in TBR lymphocytes, expressed as normalized $DioC_6(3)$ fluorescence F/F_{CCCP} (Fig. 6, white bars). The addition of oligomycin increased $\Delta\Psi_m$ of TBR mitochondria to the same level as controls, suggesting the decreased $\Delta\Psi_m$ was attributable to enhanced oxidative phosphorylation. Indeed, higher of oxygen consumption rates were observed in TBR (Fig. 7B) mitochondria relative to controls (Fig. 7A), in a manner sensitve to oligomycin. Verapamil

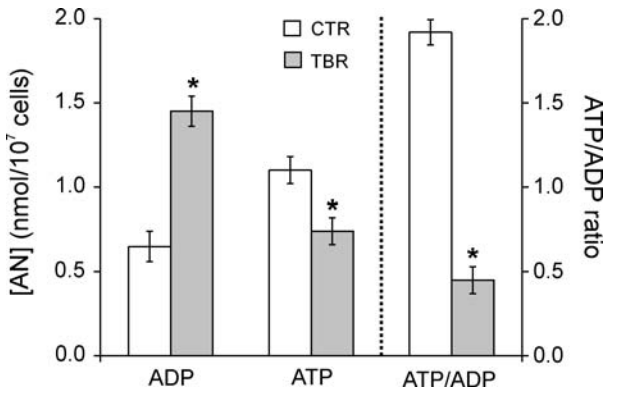

Fig. 5 Lymphocyte activation changes cellular high-energy phosphate contents. Adenine nucleotides (AN) in spleen lymphocytes (10^8 cells) isolated from CTR (*white bars*) and TBR (*gray bars*) were quantified using anion-pair-reversed-phase chromatography. Bars represent means ± SEM of five independent experiments. $^*p < 0.001$ versus CTR

restored $\Delta\Psi_m$ and respiration to control levels in TBR lymphocyte mitochondria (Fig. 7C), suggesting that Ca^{2+} entry into the cytosol and thereby to mitochondria underlies the stimulation of oxidative phosphorylation.

TBR spleen lymphocytes present enhanced NADPH oxidase-dependent ROS production

ROS production, measured by following H_2DCF oxidation, was higher in TBR lymphocytes than in controls (Fig. 8A,

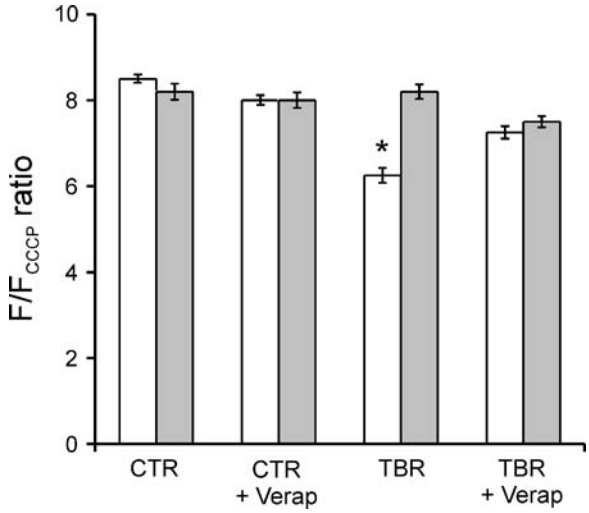

Fig. 6 Mitochondrial electrical membrane potentials are decreased by lymphocyte activation due to oxidative phosphorylation. The ratio of $DioC_6(3)$ fluorescence in the absence and in the presence of 50 μM CCCP in spleen lymphocytes (10^6 cells/mL) was measured to estimate changes in $\Delta\Psi_m$. Bars represent means ± SEM of five independent experiments performed in the absence (*white bars*) or in the presence of 1 μM oligomycin (*gray bars*) using lymphocytes isolated from CTR, CTR + Verap, TBR, and TBR + Verap. $^*p < 0.001$ versus all other experimental groups

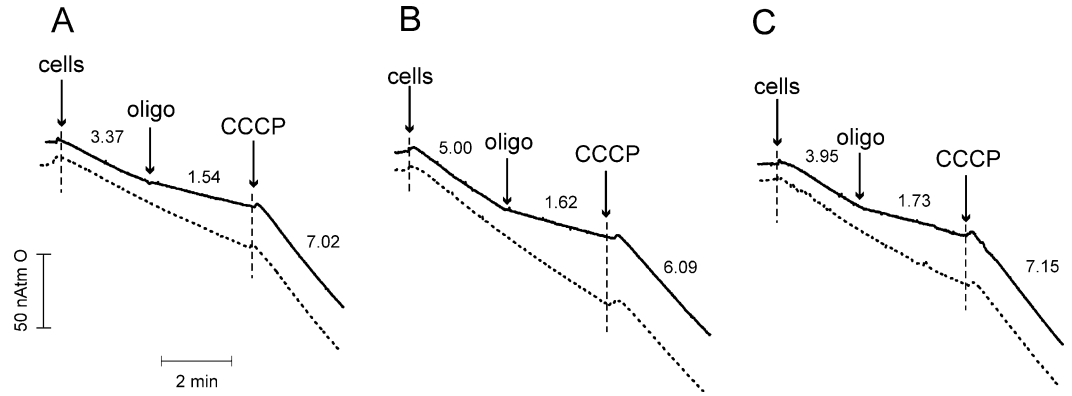

Fig. 7 Oxygen consumption is increased by lymphocyte activation in a manner dependant on oxidative phosphorylation. Spleen lymphocytes were isolated from CTR (A), TBR (B), and TBR + Verap (C). The *arrows* indicate additions of 15×10^6 lymphocytes (cells), 1 μM oligomycin (oligo) and 2 μM CCCP (*solid trace*). *Dotted traces* represent the respective experiments omitting the addition of oligomycin. Results are the representative of five independent experiments. The numbers above the lines indicate respiratory rates in spleen lymphocytes

lines *a* and *d*, respectively). The presence of DPI, an inhibitor of the NADPH oxidase, decreased the ROS production in TBR lymphocytes almost to the level of the controls (line *b*), indicating that the increased ROS release is due to NADPH oxidase activity and not mitochondrial activity. ROS production in TBR lymphocytes treated with verapamil was similar to controls (line *c*), demonstrating that increased intracellular Ca^{2+} is necessary for NADPH oxidase activation. Similar results were observed when $O_2^{\cdot -}$ production was measured by following DHE oxidation (Fig. 8B).

UCP-2 levels are elevated in TBR lymphocytes

Figure 9 shows that UCP-2 protein levels are higher in TBR lymphocytes. This finding is compatible with the induction of UCP-2 expression by high levels of ROS, as described

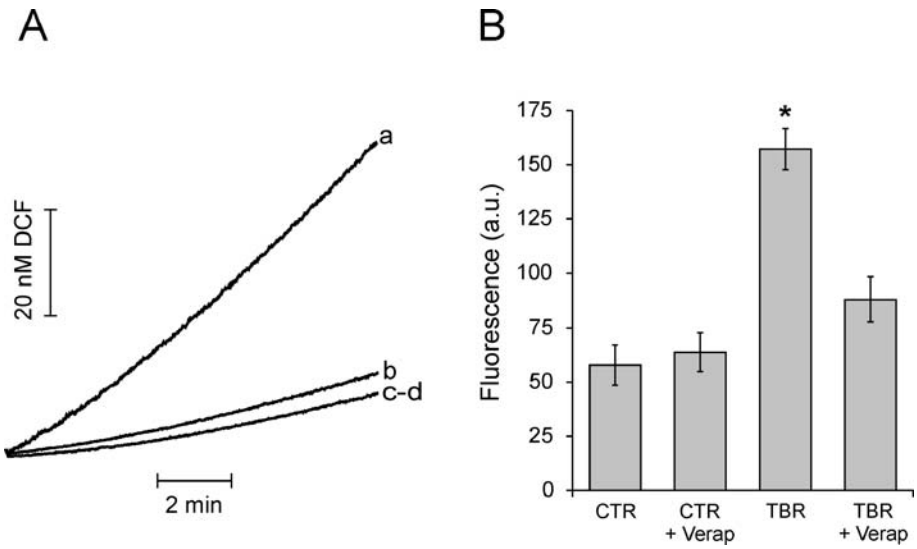

Fig. 8 ROS production by activated lymphocytes is sensitive to DPI and verapamil. (A) ROS production by spleen lymphocytes was detected fluorometrically by following H_2DCF oxidation to DCF. *Traces a* and *c* represent ROS production by spleen lymphocytes from TBR and CTR, respectively. *Trace b* represents ROS production by lymphocytes from TBR incubated in the presence of 10 μM DPI. *Trace d* represents ROS production by spleen lymphocytes from TBR + Verap. (B) Superoxide production by spleen lymphocytes (10^6 cells/mL) monitored using DHE fluorescence detected by flow cytometry. Spleen lymphocytes were incubated in the presence of 3 μM DHE at 37°C in RPMI 1640 medium for 1 h before fluorescence acquisition in a flow cytometer. Bars represent means ± SEM of 5 independent experiments. $^*p < 0.001$ versus all other experimental groups (a.u.: arbitrary units)

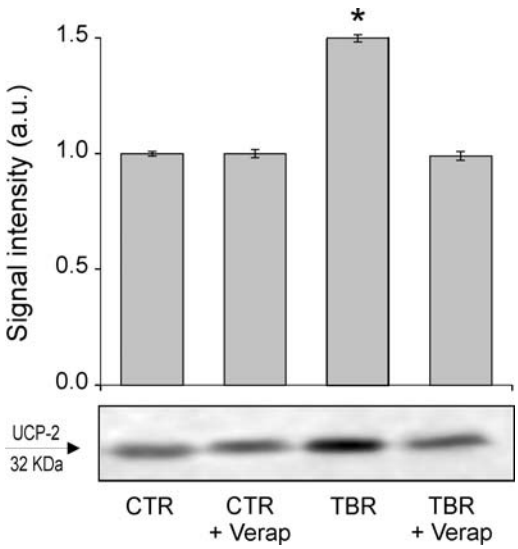

Fig. 9 UCP-2 protein levels are enhanced in TBR lymphocytes. UCP-2 levels were detected in electrophoretically separated samples of 100 μg total lymphocyte protein, using polyclonal anti-UCP-2 antibodies. Densitometric analysis (*upper panel*) was expressed as means ± SEM of five independent experiments. The *lower panel* represents a representative immunoblot. $^{*}p < 0.001$ versus all other experimental groups

previously (Echtay et al., 2002). The increased accumulation of UCP-2 was not observed in spleen lymphocytes isolated from verapamil-treated TBR (Fig. 9).

Discussion

The present study analyzed changes in intracellular Ca^{2+} levels, cellular ROS production and mitochondrial oxidative metabolism in isolated rat spleen lymphocytes during the immune response to ascitic Walker 256 tumor development. The elevated production of IL-2 and ROS and the high levels of pPKC in TBR spleen lymphocytes support the concept that the development of Walker 256 tumor induces lymphocyte activation mediated by a verapamil-sensitive increase in intracellular Ca^{2+} (Fig. 10).

The present data also demonstrate that mitochondrial Ca^{2+} levels increase in response to high cytosolic Ca^{2+}. This may activate pyruvate, isocitrate and 2-oxoglutarate Ca^{2+}-dependent dehydrogenases (McCormack and Denton, 1993) providing reducing equivalents for the respiratory chain and supporting the high ATP demand of lymphocyte activation. The high energy demand by this process was evidenced by lower ATP/ADP ratios observed in TBR lymphocytes. Indeed, the inhibition of the F_1F_0-ATP synthase by oligomycin caused restoration of $\Delta\Psi_m$ and decreased the rate of respiration by TBR lymphocytes, confirming that the Ca^{2+} signal combined with the low ATP/ADP ratio stimulated oxidative phosphorylation in these cells. This enhanced energy metabolism in TBR spleen lymphocytes can also explain their higher utilization of glucose, pyruvate and glutamine, as reported by Fernandes et al. (1994).

With respect to the condition of oxidative stress associated with lymphocyte activation, experimental evidence suggests that the engagement of T cell receptor induces rapid production of ROS (Williams and Kwon, 2004). The present results demonstrate that higher ROS production by activated spleen lymphocytes during the development of Walker tumor cells is Ca^{2+}-dependent and that the NADPH oxidase and not mitochondria is the prevalent source of these species. As a matter of fact, the high rates of oxidative phosphorylation in the TBR lymphocytes are compatible with a low rate of ROS generation by mitochondria as will be discussed later.

Concerning the viability of the lymphocytes during the activation process, it is known that sustained high levels of cytosolic Ca^{2+} and ROS increase the propensity to open the mitochondrial permeability transition pore (Kowaltowski et al., 2001), an event that may lead to cell death (Kim et al., 2003). Therefore, to accomplish their imune functions, these lymphocytes should be protected against mitochondrial dysfunction. Indeed, this occurs and was illustrated in the experiments presented in Fig. 4, showing that TBR mitochondria are resistant to Ca^{2+}-induced MPT. We propose that the accumulation of UCP-2, Bcl-2 and possibly of other anti-apoptotic factors confers mitochondrial resistance against MPT and drives the cell fate toward proliferation.

An interesting point that the present results permit to address is the concept that increased metabolic turnover leads to high production of ROS by mitochondria. This was not observed during lymphocyte activation (Fig. 8). Certainly, the high respiratory rates induced by stimulated oxidative phosphorylation or by UCPs lead to oxidized respiratory chain components. This change in redox state decreases $O_2^{\cdot -}$ generation by lowering oxygen tension in the mitochondrial microenvironment and preventing one-electron reduction of O_2 by complexes I and III (Turrens and Boveris, 1980). Thus, a decreased rate of ROS generation by mitochondria decreases the possibility of MPT opening (Kowaltowski et al., 2001; Zoratti and Szabo, 1995) and renders the mitochondrial antioxidant systems with maximal capacity to detoxify cytosolic ROS able to reach the organelle.

In conclusion, the results presented show an important relationship between intracellular Ca^{2+} homeostasis and mitochondrial bioenergetics in the process of lymphocyte activation (Fig. 10). The increase in cytosolic free Ca^{2+} concentrations leads to ROS generation by the NADPH oxidase. Accumulation of UCP-2, in addition to high rates of oxidative phosphorylation, maintain ROS generation by mitochondria at low levels, thus protecting these organelles

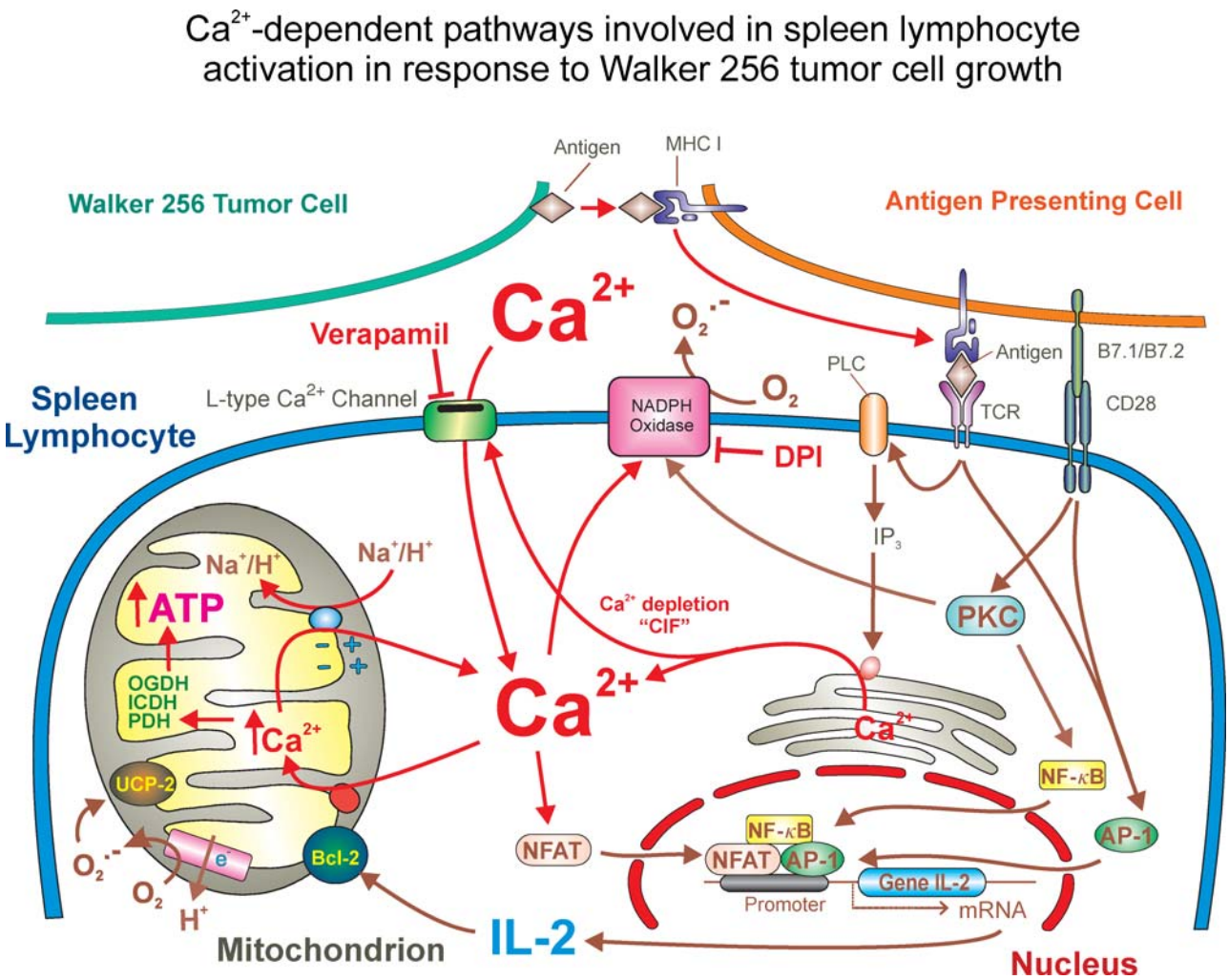

Fig. 10 Scheme summarizing Ca^{2+}-dependent pathways involved in spleen lymphocyte activation in response to Walker 256 tumor cell growth. Activation of lymphocytes in response to Walker tumor cells requires T-cell recognition of specific antigens by the interaction of the T-lymphocyte receptor (TCR) and Major Histocompatibility Complex (MHC) on antigen-presenting cells and co-stimulatory signals (B7.1/B7.2 CD28). TCR engagement induces Ca^{2+} entry through L-type plasma membrane Ca^{2+} channels sensitive to dihydropyridines (verapamil). These Ca^{2+} channels are activated by IP_3-mediated depletion of cytosolic Ca^{2+}. The elevation of mitochondrial Ca^{2+} activates Ca^{2+}-dependent dehydrogenases linked to the Krebs cycle (2-oxoglutarate dehydrogenase (OGDH); isocitrate dehydrogenase (ICDH); pyruvate dehydrogenase (PDH)) providing reducing equivalents to the respiratory chain to support a stimulated ATP demand for the process of lymphocyte activation. Ca^{2+} also activates a nuclear transcription factor NF-κB that together with nuclear factors NFAT and AP-1, activated by co-stimulatory pathway, induce the production of interleukin-2 (IL-2). IL-2 promotes lymphocyte activation and inhibits cell death by activating Bcl-2 in mitochondria. Co-stimulatory pathway also activates diphenyleneiodonium chloride (DPI)-sensitive NADPH oxidase via protein kinase C (PKC). The elevated levels of reactive oxygen species (mainly $O_2^{\cdot -}$) induce the accumulation of UCP-2 in mitochondria

against the damaging effects promoted by the combination of high $[Ca^{2+}]_{mit}$ plus ROS. This effect is probably potentiated by the accumulation of the anti-apoptotic protein Bcl-2.

Acknowledgements We thank Dr. Alicia Kowaltowski for critical reading of the manuscript and Edilene S. Siqueira and Elisângela J. Gomes for excellent technical assistance. This work was supported by Fundação de Amparo à Pesquisa do Estado de São Paulo (FAPESP), Conselho Nacional de Desenvolvimento Científico e Tecnológico (CNPq) and Coordenação de Aperfeiçoamento de Pessoal de Nível Superior (CAPES).

Bibliography

Akerman KE, Wikstron KF (1976) FEBS Lett 68:191–197
Allen RG, Tresini M (2000) Free Radic Biol Med 28:463–499
Arsenijevic D, Onuma H, Pecqueur C, et al (2000) Nat Genet 26:435–439
Barja G (2002) Ageing Res Rev 1:397–411
Birx DL, Berger M, Fleisher TA (1984) J Immunol 133:2904–2909
Boveris A, Fraga CG (2004) Mol Aspects Med 25:1–4
Böyum A (1968) Scand J Clin Lab Invest 21:31–89
Crompton M, Ellinger H, Costi A (1988) Biochem J 255:357–360

De Souza CT, Gasparetti AL, Pereira-da-Silva M, et al (2003) Diabetologia 46:1522–1531
Dröge W (2002) Physiol Rev 82:47–95
Echtay KS, Roussel D, St-Pierre J, et al (2002) Nature 415:96–99
Fernandes LC, Marques-da-Costa MM, Curi R (1994) Braz J Med Biol Res 27:2539–2543
Ferranti R, da Silva MM, Kowaltowski AJ (2003) FEBS Lett 536:51–55
Finkel T, Holbrook NJ (2000) Nature 408:239–247
Fiskum G, Craig SW, Decker GL, et al (1980) Proc Natl Acad Sci USA 77:3430–3434
Fontayne A, Dang PM, Gougerot-Pocidalo MA, et al (2002) Biochemistry 41:7743–7750
Halliwell B, Gutteridge JMC (1999) In Free Radicals in Biology and Medicine, 3rd edn (Halliwell B, Gutteridge JMC, eds), Oxford University Press, New York
Horvath TL, Diano S, Miyamoto S, et al (2003) Int J Obes Relat Metab Disord 27:433–442
Kim JS, He L, Lemasters JJ (2003) Biochem Biophys Res Commun 304:463–470
Kowaltowski AJ, Costa AD, Vercesi AE (1998) FEBS Lett 27:213–216
Kowaltowski AJ, Castilho RF, Vercesi AE (2001) FEBS Lett 495:12–15
Lewis RS (2001) Annu Rev Immunol 19:497–521
Ma P, Magut M, Faller DV, et al (2002) Cell Signal 14:849–859
Maciel EN, Vercesi AE, Castilho RF (2001) J Neurochem 79:1237–1245
Manfredi G, Yang L, Gajewski CD, et al (2002) Methods 26:317–326
Mather MW, Rottenberg H (2002) Mech Ageing Dev 123:707–724
Mattiasson G, Shamloo M, Gido G, et al (2003) Nat Med 91:1062–1068
McCormack JG, Denton RM (1993) Dev Neurosci 3–5:165–173
Metha A, Shaha C (2004) J Biol Chem 279:11798–11813
Michalek J, Buchler T, Hajek R (2004) Physiol Res 53:463–469
Negre-Salvayre A, Hirtz C, Carrera G, et al (1997) FASEB J 11:809–815
Park JW, Hoyal CR, Benna JE, et al (1997) J Biol Chem 272:11035–1143
Reth M (2002) Nat Immunol 3:1129–1134
Rottenberg H, Wu S (1998) Biochim Biophys Acta 1404:393–404
Tsien RY (1998) TINS 10:419–424
Turrens JF, Boveris A (1980) Biochem J 191:421–427
Williams MS, Kwon J (2004) Free Radic Biol Med 37:1144–1151
Zoratti M, Szabo I (1995) Biochim Biophys Acta 1241:139–176